Comparison of different liquefaction assessment methods with data from the 2010-2011 Canterbury Earthquake Sequence

S. Bertelli, S. Lopez-Querol & T. Rossetto
Department of Civil, Environmental and Geomatic Engineering, University College London, London, UK

S. Giovinazzi
Department of Civil and Natural Resources Engineering, University of Canterbury, Christchurch, NZ

L. Wotherspoon
Department of Civil and Environmental Engineering, University of Auckland, Auckland, NZ

R. Ruiter
Chorus, Christchurch, New Zealand

ABSTRACT: Soil liquefaction has caused substantial infrastructure damage in recent earthquakes. For instance, during the 2010-2011 Canterbury Earthquake Sequence (CES), in New Zealand, liquefaction-induced damage to buried cables resulted in service interruption of the telecommunication network. Being part of a broader investigation of the seismic risk of buried infrastructure, this paper aims to investigate the geotechnical data collected after the CES. First, using geotechnical information published in the New Zealand Geotechnical database (NZGD), a comparison between several semi-empirical liquefaction triggering assessment methods available in the literature is carried. Then, using a FLAC software, different soil profiles are analysed adopting the Martin *et al.*(1975) constitutive model for the sandy soil behaviour, which takes into account the accumulated volumetric strains with the cyclic loading. Finally, the numerical simulation results are compared with the ones obtained from the empirical analysis, the existing liquefaction investigations maps and field observations collected in the aftermath of the sequence.

1 INTRODUCTION

Soil liquefaction is one of the main earthquake-related hazards. Liquefaction manifestations include a variety of phenomena in which saturated soils lose strength due to the generation of excess of pore water pressures as a result of ground shaking (Kramer, 1996). The resulting vertical settlements and lateral spreading can cause severe damage to buried infrastructure systems as demonstrated in the recent seismic events (e.g. 2018 in Indonesia, 2011 in Tohoku-Japan, and the 2010-2011 Canterbury Earthquake Sequence (CES) in Christchurch, New Zealand).

Despite the relevance of liquefaction effects, the state-of-practice procedure for the assessment of liquefaction potential is based on a simplified procedure of three main phases (Bird *et al.*, 2006). First, the soil's liquefaction susceptibility examined through qualitative screening criteria of the ground condition such as the ones proposed by Bray & Sancio (2006). Then, the likelihood of liquefaction being triggered in a soil layer by a given seismic event is assessed based on the soil susceptibility and specific earthquake-parameters. Lastly, the severity of the manifestation of liquefaction at the ground surface can be defined using metrics such as the liquefaction-induced permanent ground deformations (PGDf), (Bird *et al.*, 2006; Kongar *et al.*, 2017). Regarding triggering, this is commonly established through a semi-empirical procedure first presented in the early 1970s (Seed & Idriss, 1971). Since its introduction, several variations have been proposed based on back-analyses of case studies. These semi-empirical relationships relate liquefaction triggering to a number of soil parameters determined through different field tests (e.g. Standard Penetration Test, SPT, Cone Penetration Test, CPT, and shear wave velocity measurements, Vs) (Youd & Idriss, 2001). In contrast, numerical models require more detailed site-specific geotechnical data and laboratory tests to be calibrated, and as such are less appropriate for regional-scale analysis (López-Querol, 2006).

The CES which struck Christchurch, the third most populated city in New Zealand, can be taken as a key case-study for the infrastructure vulnerability to liquefaction-induced damage. The

seismic sequence was characterised by four medium magnitude earthquakes within 15 months. Among them, the 22nd of February 2011 (Mw=6.2), located just 6 km from the city centre, is one of the most extensive liquefaction manifestation events on record (Maurer *et al.*, 2014). This earthquake caused the most severe and widespread damage to the telecommunication system due to liquefaction in roughly half of the city's developed land. For instance, the Telecom NZ investigations report (2011) describes utility holes partially floated out of the ground or filled with water in areas where there was severe liquefaction.

Although liquefaction has not been recorded in Christchurch before the CES, its high hazard was long-established due to its geomorphological setting (Bastin, 2016). Being placed on the Pacific coast and among the Heathcote, Avon, and Waimakariri Rivers, the city is characterised by a shallow groundwater table (GWT = 1-2 m) and loose, low-plasticity, Holocene alluvial deposit soils, which result in very high liquefaction susceptibilities (Maurer *et al.*, 2014). These features have been confirmed by an unprecedented number of detailed geotechnical data collected and made publically available through the New Zealand Geotechnical Database (NZGD) in the aftermath of the CES (Murahidy *et al.*, 2012). The dataset has been used to develop hazard maps through the previously mentioned simplified liquefaction triggering assessment models, these have been observed to result in either over-conservative or unconservative predictions when compared with the reconnaissance observation maps (e.g. Maurer *et al.*, 2014; Green *et al.*, 2014). Relatively less attention has been given to numerical models at this location (e.g. Beyzaei, 2017).

This paper provides a first step in understanding the liquefaction-induced damage on the telecommunication system network. It aims to compare existing different liquefaction triggering models, both semi-empirical and analytical, to identify the best one according to the observed damage. In the following, a brief overview of the semi-empirical methods and the data adopted for the computation are presented. The results of the analyses from a geographical point of view and a comparison between the different methodologies are then discussed, with consideration made on the adequacy of the state-of-practice semi-empirical approach for assessing the potential of liquefaction manifestations in Christchurch. The paper concludes by presenting numerical simulations at few locations in Christchurch, carried out with FLAC, in which the sandy soil is modelled with Martin *et al.* (1975) model. Simplified soil profiles are adopted and subjected to the Christchurch earthquake, to numerically simulate the liquefaction potential, and these are compared to the semi-empirical analyses and site observations.

2 DATA AND METHODOLOGY

This section provides an overview of the procedure used to identify the best semi-empirical liquefaction triggering assessment model. First, a concise explanation is provided of how the liquefaction potential is calculated and the different models selected. This is followed by a description of the geotechnical dataset adopted as inputs for the liquefaction estimation and the liquefaction observation maps from CES used for comparison. The section concludes with the definition of the statistical method used to evaluate the best semi-empirical model.

2.1 *Liquefaction potential index evaluation*

In engineering practice, the triggering liquefaction assessment is commonly evaluated from in-situ tests adopting the stress-based methodology first derived by Seed & Idriss (1971). This approach consists in comparing the earthquake-induced cyclic stress ratios (CSR), with the cyclic resistance ratios (CRR) of the soil to derive a Factor of Safety (FS) against liquefaction triggering for a soil layer at depth z. Liquefaction is predicted to occur if FS is less than 1. This methodology was standardised in Youd & Idriss (2001), and later updated by Moss *et al.* (2006), Idriss & Boulanger (2008), and Boulanger & Idriss (2014).

In this methodology, the CSR represents the seismic demand on a soil layer at a depth z. It is estimated considering the peak ground acceleration (PGA) at the ground surface generated by the earthquake and depends on the total and effective vertical overburden stresses. This value is then corrected through a stress reduction coefficient r_d, which accounts for the dynamic response of the soil profile (Youd & Idriss, 2001; Idriss & Boulanger, 2008; Boulanger & Idriss, 2014). The CRR depends on the soil properties and represents the ability of the soil profile to withstand the

load. Generally, it is calculated from the blow-count value (N-value) or the cone resistance (q_c) obtained from the SPT or CPT tests, respectively. These values need to be corrected for the overburden stress and atmospheric pressure. The q_c must additionally be normalised to account for the effects of non-plastic fines content on the liquefaction resistance taking into account the Soil Behaviour Type Index (I_c), (Youd & Idriss, 2001). For this purpose, the original methodology has been improved with the introduction of an iterative procedure (Moss *et al.*, 2006; Idriss & Boulanger, 2008; Boulanger & Idriss, 2014). The CRR is also influenced by the duration of seismic event, which is considered throught an earthquake magnitude scaling factor (MSF). Indeed, CRR is usually calculated using as reference conditions a 7.5 moment magnitude earthquake and effective vertical stress of 1 atm. Thus, it needs to be scaled in order to take into account different sites and event magnitudes through MSFs such as the ones formulated by Idriss (1995), Andrus & Stokoe (1997), Moss *et al.* (2006), Idriss & Boulanger (2008), Boulanger & Idriss (2014).

The FS determined through these different models forecast the triggering of liquefaction just at a specific depth z. The FS can not predict the severity of liquefaction manifestation at the surface which is the one directly linked to liquefaction-induced damage. Therefore, to better characterise the damage potential, Iwasaki *et al.* (1978) proposed an extension of this approach through the Liquefaction Potential Index (LPI). The LPI assumes that the likelihood of liquefaction manifestation at the ground surface is an integral function of the FS for each soil layer within the upper 20 m of the soil profile as defined in Eq.(1):

$$LPI = \int_0^{20m} F(10 - 0.5z)dz \quad (1)$$

where $F = 1 - FS$ for a single soil layer. Using SPT data from a collection of 45 different sites in Japan, Iwasaki *et al.* (1978) calibrated the LPI model and suggested that liquefaction risk should be assumed very low for $LPI = 0$; low for $0 < LPI \leq 5$; high for $5 < LPI \leq 15$; and very high for $LPI > 15$. These parameters for liquefaction hazard assessment are referred to herein as the Iwasaki Criterion.

Thirteen different models have been selected to assess the best SPT- or CPT-based simplified liquefaction evaluation procedures (Table 1). Regarding the SPT-based relationships, the selection includes a combination of four models from Youd & Idriss (2001) with MSF from Idriss (1995) or Andrus & Stokoe (1997), and reduction coefficients r_d from Blake (1996) or Idriss (1999), respectively as reported in Youd & Idriss (2001) and Idriss & Boulanger (2008); then the Idriss & Boulanger (2008)'s model, and the Boulanger & Idriss (2014) one. Similarly, the same models and combinations of parameters are selected for the CPT-based relationships, with the only addition of the Moss *et al.* (2006) procedure. It is noted that different relationships from different authors have not been combined with the only exception of the model of Youd & Idriss (2001) where the different alternatives have been made available by the authors themselves.

Table 1. Liquefaction prediction models tested, with reduction coefficient r_d and MSF combinations (after Youd & Idriss, 2001; Idriss & Boulanger, 2008; Boulanger & Idriss, 2014).

Model	Test	Model	r_d	MSF
SPT_YEA01a	SPT	Youd & Idriss (2001)	Blake (1996)	Idriss (1995 in Youd & Idriss, 2001)
SPT_YEA01b	SPT	Youd & Idriss (2001)	Blake (1996)	Andrus & Stokoe (1997)
SPT_YEA01c	SPT	Youd & Idriss (2001)	Idriss (1999)	Idriss (1995 in Youd & Idriss, 2001)
SPT_YEA01d	SPT	Youd & Idriss (2001)	Idriss (1999)	Andrus & Stokoe (1997)
SPT_I&B08	SPT	Idriss & Boulanger (2008)	-	-
SPT_B&I14	SPT	Boulanger & Idriss (2014)	-	-
CPT_YEA01a	CPT	Youd & Idriss (2001)	Blake (1996)	Idriss (1995 in Youd & Idriss, 2001)
CPT_YEA01b	CPT	Youd & Idriss (2001)	Blake (1996)	Andrus & Stokoe (1997)
CPT_YEA01c	CPT	Youd & Idriss (2001)	Idriss (1999)	Idriss (1995 in Youd & Idriss, 2001)
CPT_YEA01d	CPT	Youd & Idriss (2001)	Idriss (1999)	Andrus & Stokoe (1997)
CPT_MEA06	CPT	Moss *et al.* (2006)	-	-
CPT_I&B08	CPT	Idriss & Boulanger (2008)	-	-
CPT_B&I14	CPT	Boulanger & Idriss (2014)	-	-

2.2 *Data for model development*

Given the severity and size of liquefaction manifestations, the Canterbury earthquake offers a unique opportunity as a back-analysis case study. In the aftermath of the event, an in-depth soil

characterization programme was conducted, wherein more than 10,000 SPT and CPT tests have been performed and made available through the NZGD. Through this dataset, approximately 90 sites spread around the entire municipal territory are selected in the current research for possible analysis. The selection is based on the proximity of these sites to ground motions recording stations, the availability of both SPT and CPT soundings in the same location, and piezometer readings for the estimation of the GWT. The termination depth and the site location of the soundings are then cross-referenced, and tests with abnormal shallow termination (less than 10 m) are removed from the dataset. In total, only 54 high-quality sites are selected to be analysed through the aforementioned semi-empirical models, and two of these locations are considered for further numerical analyses (Fig. 1).

Regarding the values required for the computation of the FS, a spatial PGA map developed following the Bradley (2013) procedure and available on the NZGD is adopted for the estimation of the PGA at each site (NZGD, 2015). Soil unit weights are assumed to be 17 kN/m3 above the GWT, and 19.5 kN/m3 below the GWT as suggested by Wotherspoon *et al.* (2014). In the LPI analyses through the CPT soundings, layers are assumed to be potentially liquefiable if the soil behaviour type index I_c is less than 2.6, (Robertson & Wride, 1998). For the SPT estimates, the potentially liquefiable layers are identified from fine contents data from laboratory analysis.

Finally, to estimate the sensitivity of the LPI to the local conditions, low and high GWT depth are estimated based on piezometer readings, interfered with CPT pore water pressure measurements, and compared with published GWT maps (NZGD, 2013). GWT levels are variable in Christchurch, with generally shallow depths around 0-2 m in the eastern suburbs and up to 4 m in the western ones, which seasonally fluctuate by around 1 meter. The consequences of GWT level variations on the LPI estimations are discussed later in this paper.

2.3 *Observed Liquefaction Severity*

One of the advantages of the availability of detailed liquefaction data from the CES sequence is the possibility of relating the computed LPI method results to observed liquefaction data, for the identification of possible biases in the estimation procedures. The best approach for a comparison would be a direct inspection of the site locations to examine the severity of liquefaction, but this is not feasible at the time of the current research. Instead, it is possible to use published maps on the NZGD (2012, 2013).

In particular, two main surface liquefaction observation data can be adopted. The first source is a regional-scale map displaying the extent of ejected liquefied material interpreted from aerial photography (NZGD, 2012). This map is then cross-referenced with property and road observation severity maps (NZGD, 2013). These second sources have been developed through on-foot rapid inspections and, hence, offer more reliable information of evidence and quantity of ejected material which was visible at the surface. However, the classification used in these maps describes the predominant damage mechanism and manifestation of liquefaction, distinguishing between "liquefaction" and "lateral spreading" and, hence, misinterpreting the widely accepted definition of liquefaction (Kramer, 1996). Thus, this second source is taken as a reference for the comparison with the computed LPI model results given that they rely on direct site inspections, but the classification adopted is reinterpreted as detailed in the following section.

2.4 *The best model assessment procedure*

In order to assess the validity of the prediction of liquefaction occurrence, it is necessary to establish a correspondence between the calculated LPI values from the implemented semi-empirical models and the aftermentioned classification in the observation maps. Regarding the LPI models, a threshold value for the liquefaction manifestation is adopted according to the Iwasaki Criterion ($LPI \leq 5$) so that the occurrence of liquefaction at a site is predicted if the LPI value is lower than the threshold, reducing the prediction of liquefaction occurrence to a binary system. Similarly, the classification used in the observation maps is reinterpreted as "Liquefaction" or "No liquefaction" simply by matching names; "no liquefaction" and "marginal liquefaction" are mapped as negative results of liquefaction occurrence, whilst all other classes as assumed as positive occurrences of liquefaction.

The binary classification allows statistical testing of the performance of each model through a

confusion matrix approach (Berrar, 2018). In this approach, each pair of observation-prediction case can be classified as True-Positive (TP), True-Negatives (TN), False-Positive (FP), and False-Negative (FN), as represented in Fig.1. Based on this classification, several performance parameters are examined to evaluate the quality of each semi-empirical method. In particular, the accuracy (A_c) represents the ratio of the correctly predicted liquefaction or non-liquefaction pairs to all the observed cases in the dataset; the sensitivity (True Positive Rate, TPR) is the ratio of true positive predictions to the observed liquefaction cases; and the specificity (True Negative Rate, TNR) is the proportion of true negative predictions to observed no-liquefaction cases. To facilitate the assessment, these parameters are combined into the F-measure (F1), an evaluation metric which combines TPR with the proportion of correctly predicted liquefaction cases to all the predicted liquefaction, and Matthews Correlation Coefficient (MCC), a measure that balances prediction TPR and TNR (Berrar, 2018). Accordingly, the best model would have high A_c, TPR and TNR scores, an F_1 > 0.5 and a positive MCC value.

3 SPATIAL ANALYSIS AND TEST DIAGNOSIS RESULTS OF LPI MODELS

Preliminary spatial analyses are carried out to evaluate the LPI performance of the adopted methods. The resulting LPI values are assessed assuming a threshold $LPI \leq 5$ for the occurrence of liquefaction, and compared with observation data. Results are grouped according to the TP, TN, FP, FN classification for the shallower GWT (Figure 1); a pie-chart representation is adopted to assess at each site location the cumulative results from the 13 different models. For instance, if the liquefaction has been observed in a site, the pie chart is "red" and "light blue" proportionally to the number of models which predict TP (liquefaction) or FN (no-liquefaction).

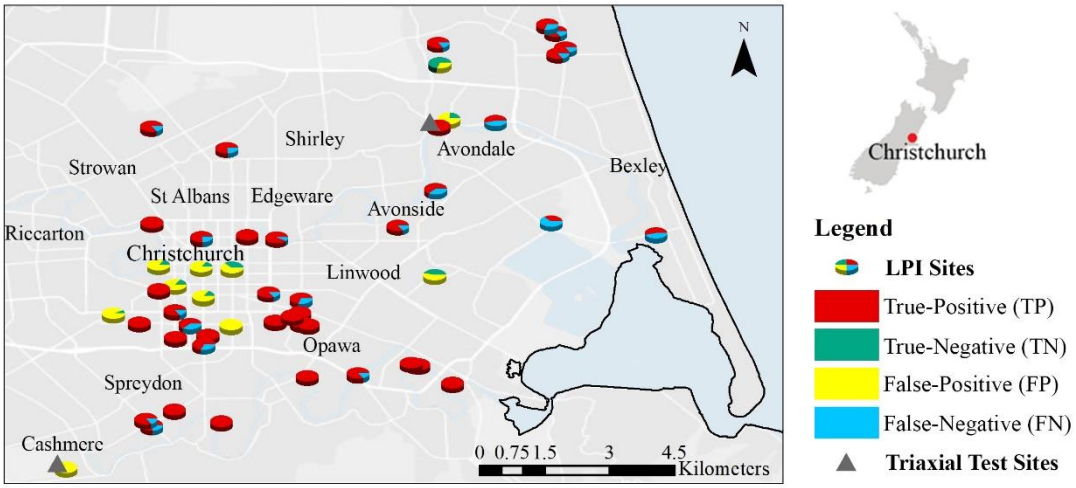

Figure 1. Comparison of the observation data with the LPI values according to the 13 different models for each site location and the shallower GWT.

It is clear from Figure 1 that there is a general overprediction of liquefaction occurrence, particularly in the western side of Christchurch. For instance, all the different LPI models result in FP for the Cashmere site. A plausible explanation might be linked to geomorphological features of the western suburbs, where the soil profiles show an increasing mix of sand, silt and gravel, especially for depths up to 10 m (Kongar *et al.*, 2017). Thus, it is possible that the calculated LPI values may indicate liquefiable soil layers when they are not, which leads to overestimation of LPI and the extent of liquefaction occurrence prediction.

The results obtained from further numerical analyses along with the corresponding statistical measures are reported in Table 2. The single most striking observation is that all models seem to present high A_c, TPR, and F_1 indifferently from the GWT level adopted and whether SPT- or CPT- based. The model which seems to perform better amongst both GWT measurements is Idriss & Boulanger (2008) CPT=based. However, the MCCs for this model are close to zeros, indicating that the model cannot effectively predict the non-liquefaction occurence, and the correlation is rather casual. Indeed, these parameters confirm the overall trend of the semi-empirical models to

overpredict liquefaction manifestations.

No significant difference in prediction is observed for the two GWT values adopted. The water level in Christchurch varies seasonally by roughly 1m, which can lead in some cases in an overprediction of liquefaction manifestation. However, this fluctuation has a limited effect on the LPI. This result is consistent with Maurer *et al.* (2014) who show that liquefaction prediction errors are unlikely to be a result of widespread GWT depth estimation or GWT fluctuation.

It is observed that all the refinements added over the years to the original Seed & Idriss (1971) formulations do not result in a significantly better prediction of liquefaction occurrence. For instance, the LPI values through the SPT-based Youd & Idriss (2001) models are not dissimilar to those obtained with the Idriss & Boulanger (2008) CPT-based approach. This may be due to all the uncertainties that have been introduced for the model development such as the soil density and the threshold values for the liquefaction assessment. In future investigations, it might be possible to use alternative LPI threshold criteria to calibrate these models, which would provide a better fit with the observation maps (e.g. Maurer *et al.*,2014; Kongar *et al.*, 2017). Nonetheless, uncertainties are an intrinsic characteristic of these semi-empirical methods which are unlikely to be solved with refinements of the existing approaches.

Table 2. Accuracy (A_c), sensitivity (TPR), specificity (TNR), F-measure (F_1), and Matthew Correlation Coefficients (MCC) for the 13 different LPI models. Min(GWT) and Max(GWT) represents the shallower and deeper water level from the ground surface.

Model	Min(GWT)					Max(GWT)				
	A_c	TPR	TNR	F_1	MCC	A_c	TPR	TNR	F_1	MCC
SPT_YEA01a	0.89	0.81	0.67	0.86	0.11	0.91	0.82	0.60	0.87	0.16
SPT_YEA01b	0.89	0.81	0.67	0.86	0.11	0.91	0.82	0.60	0.87	0.16
SPT_YEA01c	0.87	0.81	0.71	0.84	0.09	0.81	0.82	0.70	0.83	0.11
SPT_YEA01d	0.87	0.81	0.71	0.84	0.09	0.81	0.82	0.70	0.83	0.11
SPT_I&B08	0.48	0.88	0.71	0.67	0.21	0.33	0.83	0.78	0.49	0.07
SPT_B&I14	0.46	0.88	0.72	0.65	0.19	0.35	0.84	0.77	0.52	0.08
CPT_YEA01a	0.98	0.79	1.00	0.88	0.07	0.83	0.80	0.78	0.82	0.02
CPT_YEA01b	0.98	0.79	1.00	0.88	0.07	0.81	0.80	0.80	0.80	0.01
CPT_YEA01c	0.93	0.82	0.50	0.88	0.21	0.80	0.79	0.82	0.79	0.03
CPT_YEA01d	0.91	0.82	0.60	0.87	0.16	0.80	0.79	0.82	0.79	0.03
CPT_MEA06	0.89	0.77	1.00	0.81	0.18	0.65	0.83	0.74	0.74	0.11
CPT_I&B08	**0.98**	**0.79**	**1.00**	**0.88**	**0.07**	**0.93**	**0.78**	**1.00**	**0.84**	**0.14**
CPT_B&I14	0.74	0.83	0.71	0.80	0.12	0.48	0.81	0.78	0.63	0.08

4 NUMERICAL SIMULATION

To further assess the liquefaction manifestation at sites, two soil columns, representing the Cashmere and Avondale locations, have been simulated using FLAC 2D. The models consist of 6 and 7 m deep soil columns, respectively. Based on the experimental information provided by Beyzaei (2017), two types of soils have been considered. For Cashmere, the column is clayey material except for a 1 m layer of sandy soil from 3 to 4m deep; in the case of Avondale, all the material is assumed to be liquefiable sandy material. The input loading applied are those recorded in terms of PGV at the CMHS and HDPS recording stations, respectively the closest ones to the Cashmere and Avondale site, and obtained from PEER Ground motion Database. The clayey soil is assumed as Mohr-Coulomb, with c=10kPa, ϕ'=15degrees of friction, E=29MPa, υ=0.45, and permeability of 1e-12m/s. The sandy material is simulated with the Martin *et al.* (1975) law. The main parameters for these materials are E=31MPa, υ=0.2 a ϕ'=37degree, and c1=0.79, c2=0.52, c3=0.2 and c4=0.5, which represent a fairly liquifiable material. The water level is assumed 1m deep in all cases. Free field boundary conditions are implemented in the models.

The numerical simulations yield clear liquefaction of the Avondale profile to a depth of 5 m (see Figure 2a), while in Cashmere such phenomenon is localised within the sandy layer (Figure 2b), causing high ground displacement which can be understood as lateral spreading more than soil liquefaction (Figure 2.c). In contrast with the semi-empirical models, which overpredict the liquefaction manifestations at the Cashmere site, these results are in agreement with observations

and, thus, more reliable despite the huge assumptions made for the calibration of the models.

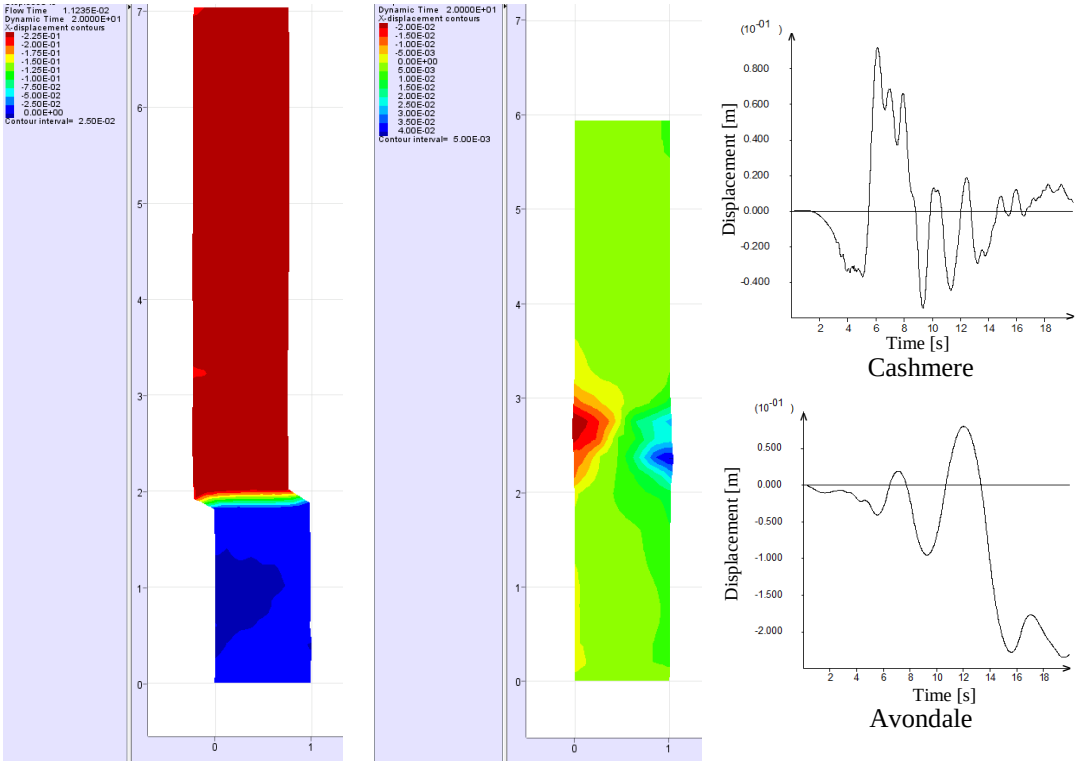

a) b) c)

Figure 2. Results of the numerical simulations. a) Final x displacements in Avondale. b) Final x displacements in Cashmere. c) Histories of x displacements on top of the soil profiles.

5 CONCLUSION

The present research compares a range of simplified semi-empirical liquefaction assessment methods available in the literature as the first step into a vulnerability assessment of the liquefaction-induced damage on telecommunication infrastructure systems. Adopting in-situ geotechnical inspections data collected in the aftermath of the 2011 Christchurch event, results show that the CPT-based LPI method proposed by Idriss & Boulanger (2008) is the best performing of the selected approaches, even though the obtained results are not dissimilar from the others models. Indeed, their ability to correctly predict liquefaction occurrence both positively and negatively is quite poor, and cannot be justified by GWT fluctuations.

Taken together, these results suggest that refinements added over the years to the original formulation of Seed & Idriss (1971) do not compensate for the intrinsic uncertainties of these models. These semi-empirical approaches are fast and straightforward to apply, but the provided liquefaction occurrence predictions are highly uncertain, hence they should not be relied upon for seismic risk assessment studies. On the contrary, numerical simulation, using a well-known state of the art constitutive model for liquefaction assessment, is in agreement with the observations, and in contradiction with the semi-empirical procedure for one of the simulated cases. These can provide an alternative to the empirical approaches in seismic risk modelling, but require more accurate site-specific geotechnical data and are hence less appropriate for regional-scale studies.

6 ACKNOWLEDGEMENTS

The authors are grateful to Myrto Papaspiliou from Willis Research Network for providing valuable remarks. Funding for this research project has been provided by QuakeCoRE, UCL CEGE Department and the Willis Research Network.

REFERENCES

Andrus, R.D. & Stokoe, K.H., 1997. *Liquefaction resistance based on shear wave velocity*. NCEER-97.

Bastin, S.H., 2016. *Liquefaction and Paleo-liquefaction in Christchurch, New Zealand*. University of Canterbury.

Berrar, D., 2018. Performance Measures for Binary Classification. *Encyclopedia of Bioinformatics and Computational Biology*, Academic Press, pages 546-560.

Beyzaei, C.Z., 2017. *Fine-Grained Soil Liquefaction Effects in Christchurch, New Zealand*. UC Berkeley.

Bird, J.F., Bommer, J.J., Crowley, H. and Pinho, R., 2006. Modelling liquefaction-induced building damage in earthquake loss estimation. *Soil Dynamics and Earthquake Engineering*, 26(1), pp.15-30.

Boulanger, R.W. & Idriss, I.M., 2014. *CPT and SPT based liquefaction triggering procedures*. Report No. UCD/CGM-14/01. Center for Geotechnical Modeling, University of California Davis, California.

Bradley, B.A., 2013. Estimation of site-specific and spatially-distributed ground motion in the Christchurch earthquakes: Application to liquefaction evaluation and ground motion selection for post-event investigation. Proc. *19th NZGS Geotechnical Symposium*. Ed. CY Chin, Queenstown.

Bray, J.D. & Sancio, R.B., 2006. Assessment of the liquefaction susceptibility of fine-grained soils. *Journal of geotechnical and geoenvironmental engineering*, 132(9), pp.1165-1177.

Green, R.A., Cubrinovski, M., Cox, B., Wood, C., Wotherspoon, L., Bradley, B. and Maurer, B., 2014. Select liquefaction case histories from the 2010–2011 Canterbury earthquake sequence. *Earthquake Spectra*, 30(1).

Idriss, I. & Boulanger, R., 2008. *Soil Liquefaction during Earthquakes*. Monograph Series: Earthquake Engineering Research Institute, Oakland, California.

Iwasaki, T., Tatsuoka, F., Tokida, K., & Yasuda, S., 1978. *A practical method for assessing soil liquefaction potential based on case studies at various sites in Japan*. Proc., 2nd Int. Conference on microzonation, National Science Foundation, Washington, D.C.

Kongar, I., Rossetto, T. and Giovinazzi, S., 2017. Evaluating simplified methods for liquefaction assessment for loss estimation. *Natural Hazards and Earth System Sciences*, *17*(5), pp.781-800.

Kramer, S.L., 1996. *Geotechnical earthquake engineering*. In prentice–Hall international series in civil engineering and engineering mechanics. Prentice-Hall, New Jersey.

López-Querol, S. & Blázquez, R., 2006. Liquefaction and cyclic mobility model for saturated granular media. *International journal for numerical and analytical methods in geomechanics*, *30*(5).

Martin, G.R., Finn, W.L. and Seed, H.B., 1975. Fundamentals of liquefaction under cyclic loading. *Journal of Geotechnical and Geoenvironmental Engineering*, *101*(ASCE# 11231 Proceeding).

Maurer, B.W., Green, R.A., Cubrinovski, M. and Bradley, B.A., 2014. Evaluation of the liquefaction potential index for assessing liquefaction hazard in Christchurch, New Zealand. *Journal of Geotechnical and Geoenvironmental Engineering*, 140(7), p.04014032.

Moss, R., Seed, R., Kayen, R., Stewart, J., Der-Kiureghian, A., & Cetin, K., 2006. CPT-Based probabilistic and deterministic assessment of in situ seismic soil liquefaction potential. *Journal of Geotechnical and Geoenvironmental Engineering*, 132(8):1032{1051.

Murahidy, K.M., Soutar, C.M., Phillips, R.A. and Fairclough, A., 2012. Post-earthquake recovery–development of a geotechnical database for Christchurch central city. In *Proceedings of the 15th world conference on earthquake engineering*, Lisbon, Portugal.

New Zealand Geotechnical Database, 2012. *Aerial Photography*, Map Layer CGD0100 - 1 June 2012, retrieved from https://www.nzgd.org.nz/

New Zealand Geotechnical Database, 2013. *Liquefaction and Lateral Spreading Observations*, Map Layer CGD0300 - 11 Feb 2013, retrieved from https://www.nzgd.org.nz/

New Zealand Geotechnical Database, 2014. Event Specific Groundwater Surface Elevations, Map Layer CGD0800 – 12 June 2014, retrieved from https://www.nzgd.org.nz/

New Zealand Geotechnical Database, 2015. Conditional PGA for Liquefaction Assessment, Map Layer CGD5110 – 30 June 2015, retrieved from https://www.nzgd.org.nz/

Robertson, P.K. & Wride, C.E., 1998. Evaluating cyclic liquefaction potential using the cone penetration test. *Canadian Geotechnical Journal*, 35(3), pp.442-459.

Seed, H.B. & Idriss, I.M., 1971. Simplified procedure for evaluating soil liquefaction potential. *Journal of Soil Mechanics & Foundations Div.*

Wotherspoon, L., Orense, R.P., Green, R., Bradley, B., Cox, B. & Wood, C., 2014. Analysis of liquefaction characteristics at Christchurch strong motion stations. *Soil Liquefaction During Recent Large-Scale Earthquakes*, London, UK, pp.33-43.

Youd, T.L. & Idriss, I.M., 2001. Liquefaction resistance of soils: summary report from the 1996 NCEER and 1998 NCEER/NSF workshops on evaluation of liquefaction resistance of soils. *Journal of geotechnical and geoenvironmental engineering*, 127(4), pp.297-313.